

Study of high frequency transient overvoltage caused by cable-transformer quarter-wave resonance

Paul Akiki, Alain Xémard, Charlotte Trouilloud, Jean-Luc Chanelière

Abstract—When the substations are separated from the overhead line by an underground cable, surge arresters are usually installed at the junction between the overhead line and the cable. Typical insulation coordination studies are conducted in order to decide if another set of surge arresters is required at the entrance of the substation. In this paper, a less classic issue is investigated. It studies the conditions of occurrence of strong overvoltages due to the interaction between a quarter-wave underground cable and the HV/MV power transformer, following a lightning strike. These overvoltages may appear on the secondary side of the transformer even if at the primary side they are well below the lightning withstand voltage of the equipment. The theoretical background is presented and the high frequency models of the system's component are detailed. In particular, a high-frequency model of the transformer is developed. An EMTP-like program is used to simulate the time domain electromagnetic behavior of the system and to investigate the different resonance frequencies. It is shown that, in configurations where the transformer is unloaded, the cable exhibits a quarter-wave behavior at specific lengths and frequencies which leads to high overvoltages. The connection of the load modifies the frequency response of the system and eliminates the risk of appearance of these critical overvoltages.

Keywords: Resonance, quarter-wave, high-frequency, overvoltage, power transformer, underground cable, EMTP

I. INTRODUCTION

LIGHTNING strikes are natural phenomena that cause high frequency voltage transients to travel along the power transmission lines. Such transients result in high overvoltage that cause insulation stress and may lead to power transformer failure. In literature, numerous experimental and theoretical investigation can be found regarding the propagation and impact of lightning overvoltage on transformers [1]-[3]. Along these studies, the specifications of mitigation equipment such as surge arresters are generally presented. They may concern traditional high-voltage systems but also modern power networks with distributed generation as wind farms and photovoltaic panels [4], [5].

The aforementioned studies focus mainly on the primary side of a single transformer with generally a transmission network formed by overhead lines. Other studies investigate the interaction in a hybrid transmission network where overhead lines and underground cables can be found [6], [7].

Resonance may appear between the cable and the transformer at certain configurations with specific cable lengths: half wavelength and quarter wavelength. Some studies investigate the electromagnetic transients in half wavelength transmission lines [8], [9].

However, much less can be found about quarter wavelength power lines and cables. The authors in [2] give the quarter resonance as an example when studying the classic case of transformer energization via a cable without detailing the phenomenon. The reference [3] studies the transients between the transformer and the power system and includes the study of the lightning overvoltage impact on transformers. Besides, it presents a subsection on the cable-transformer quarter wave resonance. However, the theoretical explanation of this phenomenon is not given explicitly and a basic example of a unit voltage step is presented to illustrate the case. In [10], the author describes the general resonance overvoltage of a cable-transformer system without presenting the quarter-wave phenomenon. In addition, the examples given in [10] focus mainly on ground faults and on the energization of the transformer.

In this paper, an extended theoretical explanation of the quarter-wave resonance along with the required conditions for this type of interaction are presented. An original case study is analyzed. It concerns a lightning strike resonant overvoltage between a quarter-wave underground cable and a HV/MV power transformer in a configuration with power towers, overhead-underground junction and surge arresters. In the studied configuration, a lightning strike causes the failure of a surge arrester located at the entrance of the substation. It is shown that a severe overvoltage may occur on the low voltage side of the unloaded transformer, even if the overvoltage on the high voltage side are well below the lightning withstand voltage of the equipment [11]. Furthermore, most of the studies found in literature uses transformers with no load condition when studying the quarter-wave resonance. In this work, the effect of the load on overvoltage reduction is analyzed.

In the next sections, the theoretical background for a quarter-wave resonance is recalled. The high frequency modeling of the studied power system is detailed. It concerns the lightning current, the electric towers, the transmission lines/cables and the power transformer. Finally, the different resonance frequencies are investigated and the influence of the quarter-wave cable length is analyzed in order to better understand its effect on the overvoltage transmitted to the LV side of the transformer. It is shown that the load of the transformer can eliminate the risk of existence of these severe overvoltages.

P. Akiki, A. Xémard, C. Trouilloud and J-L. Chanelière are with EDF, 7 boulevard Gaspard Monge, 91120, Palaiseau, France. (e-mails: paul.akiki@edf.fr, alain.xemard@edf.fr, charlotte.trouilloud@edf.fr, jean-luc.chaneliere@edf.fr).

II. THEORETICAL BACKGROUND

A. Telegraph equations

When the voltage wavelength is short compared to the length of a line, voltage and current vary along the line [12]. It is therefore not appropriate to model a transmission line by a single cell (i.e.: a single circuit with the inductance, the capacitance, the conductance and the resistor calculated for the total length of the line) connecting the generator (represented by a voltage source e and an internal impedance Z_g) to the load (represented by an impedance Z_t). Thus, each infinitesimal element (i.e. fraction of the line with infinitely small length dx) is replaced by the elementary circuit shown in Fig. 1.

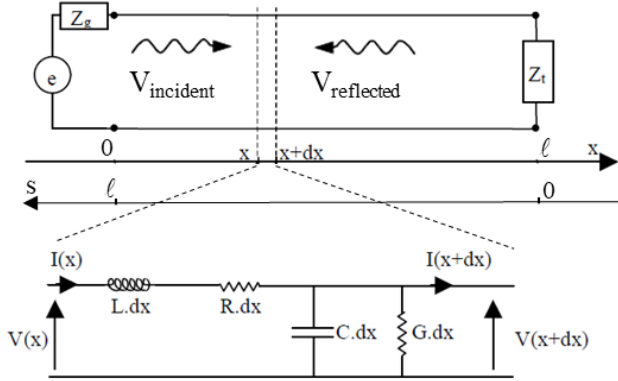


Fig. 1. Equivalent circuit for an infinitesimal element of a transmission line.

The inductance $L.dx$ represents the magnetic effects due to the passage of current in the conductors, the capacitor $C.dx$ models the capacitor made up of the two conductors brought to different potentials, the resistor $R.dx$ represents the losses by Joule effect and finally the conductance $G.dx$ represents the dielectric losses. L , C , R , G are defined by unit of length and are characteristic of the line (L in H/m, C in F/m, R in Ω/m and G in Ω^{-1}/m).

Kirchhoff's laws are applied to the elementary circuit given in Fig. 1 and sinusoidal waveforms with angular frequency ω are considered. The derivative with respect to dx yields to the so-called telegraph equations in the frequency domain:

$$\frac{d^2V}{dx^2} - ZY V(x) = 0 \quad (1)$$

$$\frac{d^2I}{dx^2} - YZ I(x) = 0 \quad (2)$$

with $Z = R + jL\omega$ and $Y = G + jC\omega$. The solutions for (1) and (2) are given by:

$$V(x, t) = (V_1 e^{-\gamma x} + V_2 e^{\gamma x}) e^{j\omega t} \quad (3)$$

$$I(x, t) = \frac{1}{Z_0} (V_1 e^{-\gamma x} - V_2 e^{\gamma x}) e^{j\omega t} \quad (4)$$

The propagation factor of the wave γ is expressed by:

$$\gamma = \alpha + j\beta = \sqrt{ZY} \quad (5)$$

where the real part α is the attenuation factor and the

imaginary part β is the propagation factor. Z_0 is the characteristic impedance of the transmission line. It is complex in the general case and varies with the frequency.

According to (3) and (4), the voltage and the current are the superposition of two attenuated traveling waves that propagate on the transmission line with opposite directions of propagation. The first going from the generator (increasing x) is called an "incident wave", while the second returning to the generator (decreasing x) is called a "reflected wave" (Fig. 1).

B. Lossless lines: reflection coefficient and impedance

The reflection coefficient Γ is defined as the ratio of the complex amplitude of the reflected wave to that of the incident wave. It is expressed by:

$$\Gamma(x) = \frac{V_{\text{reflected}}}{V_{\text{incident}}} = \frac{V_2 e^{\gamma x}}{V_1 e^{-\gamma x}} = \frac{V_2}{V_1} e^{2\gamma x} \quad (6)$$

The impedance is given by:

$$Z(x) = \frac{V(x)}{I(x)} = \frac{V_1 e^{-\gamma x} + V_2 e^{\gamma x}}{\frac{1}{Z_0} [V_1 e^{-\gamma x} - V_2 e^{\gamma x}]} \quad (7)$$

It is convenient to introduce the normalized impedance $z(x)$ defined as the ratio of the impedance $Z(x)$ to the characteristic impedance Z_0 :

$$z(x) = \frac{Z(x)}{Z_0} = \frac{1 + \Gamma(x)}{1 - \Gamma(x)} \quad (8)$$

When applying (8) at the end of the line ($x = l$), the reflection coefficient can be written as follows:

$$\Gamma(x) = \Gamma_t e^{2\gamma(x-l)} \text{ where } \Gamma_t = \Gamma(l) = \frac{V_2}{V_1} e^{2\gamma l} \quad (9)$$

Equation (9) depends on the length l of the line. However, only the distance between the load and the observation point x is important. Thus, the coordinate system is changed and the variable s is adopted which has its origin on the load and its positive direction goes towards the generator (Fig. 1). In this coordinate system, (9) can be written as follows:

$$\Gamma(s) = \Gamma_t e^{-2\gamma s} \quad (10)$$

Thus, the normalized impedance is given by:

$$z(s) = \frac{1 + \Gamma(s)}{1 - \Gamma(s)} = \frac{z_t + th(\gamma s)}{1 + z_t th(\gamma s)} \text{ with } \Gamma_t = \frac{z_t - 1}{z_t + 1} \quad (11)$$

As a simplification, losses are neglected ($R = G = 0$) which leads to an attenuation factor $\alpha = 0$. Thus, the propagation factor is given by:

$$\gamma = j\beta \text{ with } \beta = \frac{2\pi}{\lambda} \text{ and } \lambda = v/f \quad (12)$$

where λ is the wavelength, v the propagation speed of the wave and f the frequency. Substituting (12) in (11) gives the following expression for the normalized impedance:

$$z(s) = \frac{z_t + j tg(\beta s)}{1 + j z_t tg(\beta s)} \quad (13)$$

C. Quarter-wave resonance

A quarter-wave line is a line of length $\lambda/4$ where λ is given at a particular frequency. When this line is loaded by z_t , the impedance transformed by the quarter-wave line and seen at $s = \lambda/4$ is given by:

$$z\left(s = \frac{\lambda}{4}\right) = \lim_{\beta s \rightarrow \frac{\pi}{2}} \left[\frac{z_t + j \operatorname{tg}(\beta s)}{1 + j z_t \operatorname{tg}(\beta s)} \right] = \frac{1}{z_t} \quad (14)$$

Hence, the normalized impedance is inverted by a quarter-wave line.

When considering a line with an open-circuit ($z_t = \infty$), the impedance at quarter-wavelength is given by (14) and yields to:

$$z(\lambda/4) = 0 \quad (15)$$

Therefore, a quarter-wave line terminated by an open-circuit creates a short-circuit at its input. In the case of a real line with losses, the impedance at the input of the quarter-wave line is very low and the behavior is similar to a short circuit. Thus, at a distance $\lambda/4$ from the open-circuit (in the direction of the source) (see point s_0 given in Fig. 2), the impedance being very low, the current is then minimum and the voltage is maximum. At the open-circuit, the voltage sine wave is at its maximum and the current sine wave is at its minimum. This is called voltage quarter-wave resonance. This phenomenon is true for any odd multiple of the quarter-wave line i.e. for any line of length $(2k + 1) \lambda/4$ with $k = 0, 1, 2 \dots$ terminated with an open-circuit.

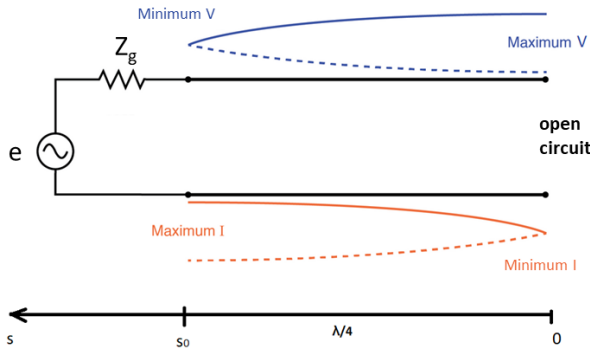


Fig. 2. Illustration of the resonance due to a quarter-wave line terminated with an open-circuit

III. DESCRIPTION OF THE STUDIED CASE

A configuration is considered in which a transmission line is connected to a Gas Insulated Substation (GIS) via an underground cable. The substation is protected against lightning by surge arresters installed at the junction between the cable and the overhead line. The GIS is connected to a HV / MV transformer with no load. The general schematic of the studied configuration is given in Fig. 3.

It is considered that a lightning strikes the overhead line and leads to the failure of an arrester. The overvoltage on the low voltage side of the transformer is studied.

Time domain electromagnetic transient calculations are performed using EMTP [13]. The models of the different components are presented in the next paragraphs [14].

A. Lightning current

The lightning strike is modeled using Heidler function [15]:

$$i(t) = \frac{i_{max}}{k} \frac{(t/\tau_1)^{10}}{1 + (t/\tau_1)^{10}} e^{-t/\tau_2} \quad (16)$$

where i_{max} is the current amplitude and k the correction factor of the current maximum. The coefficients τ_1 and τ_2 determine the decay time and the front time, respectively. In this work we consider the first negative strike with an amplitude of 100 kA. The parameters k , τ_1 and τ_2 are equal to 0.986, 1.82 μ s and 285 μ s, respectively. They are given in IEC 62305-1 [16].

B. Electric towers and GIS

The electric towers and the GIS are modeled using the constant parameters (CP) line model [17]. The towers are single phase lines with a length of 54 m connected to the ground with a 15 Ohms resistor. The GIS is considered to be a three phase line with a length of 10 m.

C. Transmission lines and cables

Frequency dependent models [18], [19] are used for the overhead transmission lines, the underground cable and the distribution cables connected to the secondary winding of the transformer. In such models, the lines/cables distributed parameters R , L , C and Z_c , presented in the previous section, vary with frequency and lead to more accurate results. In this work, the underground cable that feeds the GIS and the power transformer is of interest. Thus, its characteristics are given in TABLE I.

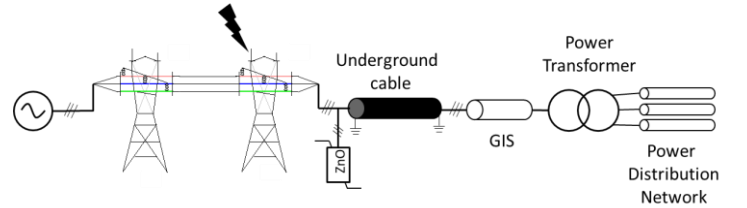


Fig. 3. General schematic of the studied case

TABLE I
UNDERGROUND CABLE MAIN CHARACTERISTICS

Cable type	Single core coaxial cable
Number of phases	3
Cable length	2 km
Outer insulation radius	45 mm
Core conductor radius	15 mm
Inner shield conductor radius	40 mm
Outer shield conductor radius	43 mm

D. Power transformer

In this paper a three phase core type power transformer is considered. Its main characteristics are given in TABLE II. Fig. 4 shows a 2D schematic of a single phase winding. Both high voltage (HV) and low voltage (LV) windings are cylindrical. A high frequency (HF) model is developed in which each winding is divided into two parts. The inductances and capacitances between these parts are taken into account. The inductance circuit is derived from the duality concept applied to the reluctance circuit of the transformer [20]. Each winding block is represented by an ideal transformer whose

primary (with number of turns equal to that of the considered block) is connected to the capacitors circuit. The secondary winding (with 1 turn) is connected to the inductors circuit which represents the magnetic couplings. The relative permeability of the magnetic circuit is considered to be infinite. Thus, the transformer model is not suitable at low frequencies.

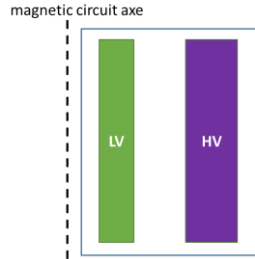


Fig. 4. Single phase 2D winding schematic

TABLE II
TRANSFORMER MAIN CHARACTERISTICS

Transformer type	Core type
Number of phases	3
Power	29 MVA
High voltage	235 kV
Low voltage	6.8 kV
Vector group	YNd11

The high frequency model of a single phase is shown in Fig. 5. The three phase transformer is obtained by coupling three single phases as wye-delta. The horizontal inductances (L_h) and vertical inductances (L_v) are given by:

$$L_h = 2 \pi \mu_0 r_m d_h / d_r \quad (17)$$

$$L_v = 2 \pi \mu_0 r_m d_r / d_h \quad (18)$$

where μ_0 is the vacuum permeability, r_m is the mean radius of the HV and LV windings, d_r is the distance between the HV and LV windings, d_h is the height of the considered block of windings.

The capacitances between HV and LV (C_{HV_LV}) and between the LV and the core (C_{LV_core}) are calculated using the equation of a cylindrical capacitor:

$$C_{HV_LV} = 2\pi\epsilon_0\epsilon_r \frac{H}{\ln(R_{HV_int}/R_{LV_ext})} \quad (19)$$

$$C_{LV_core} = 2\pi\epsilon_0\epsilon_r \frac{H}{\ln(R_{LV_int}/R_{core})} \quad (20)$$

where ϵ_0 and ϵ_r are the vacuum permittivity and relative permittivity, respectively. H is the windings height, R_{HV_int} is the HV internal radius, R_{LV_ext} is the LV external radius, R_{LV_int} is the LV internal radius and R_{core} is the core radius.

The capacitance of each high voltage block winding (C_{HV}) is calculated using the equation of a planar capacitor:

$$C_{HV} = \epsilon_0\epsilon_r \pi (R_{HV_ext}^2 - R_{HV_int}^2) / d_h \quad (21)$$

where R_{HV_ext} is the HV external radius. The capacitance of each LV block winding (C_{LV}) is obtained by replacing the subscript HV by LV. The capacitances between the HV

winding, the tank and the magnetic circuit are neglected due to their low values.

This approach was experimentally validated using a frequency response analyzer. The comparison of the HV winding admittance (Y_{11}) between the model and the measurements is given in Fig. 6. The main resonances are correctly represented with a slight frequency shift. The amplitude of the resonance are overestimated with the model because the transformer losses are neglected. Other approaches which use numerical methods to compute R, L, C and G matrices exist and are more accurate to create high frequency models. However, they require much more details about the transformer geometry and its internal winding configuration. In addition, the numerical approaches require high computational time and resources [21].

For the purpose of the study, the experimental comparison shows that the developed transformer model presents a good agreement with the measurements.

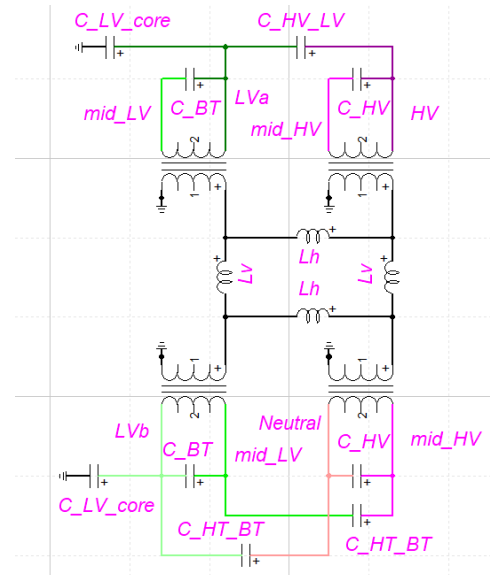


Fig. 5. Single phase high frequency model

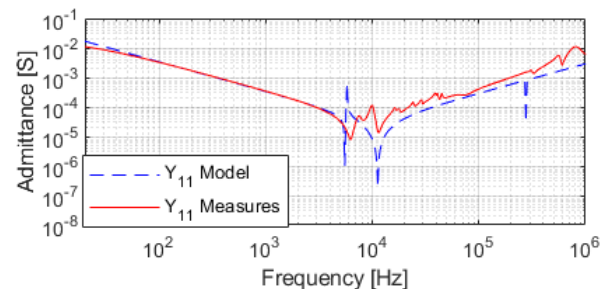


Fig. 6. Comparison of the admittance Y_{11} between the model and the measurements

IV. QUARTER-WAVE CABLE-TRANSFORMER RESONANCE

A. No-load cable frequency analysis

A frequency scan is performed on the underground cable in no-load condition. The cable length is 2 km as indicated in TABLE I. A sinusoidal voltage source with an amplitude of 1 V is used. Three cases are considered depending on the sheath grounding mode:

- Case ‘a’: sheaths on both ends of the cable are connected to the ground
- Case ‘b’: only the sheaths located on the source side are connected to the ground
- Case ‘c’: only the sheaths located on the opposite side of the source are connected to the ground

The voltage magnitude for cases ‘a’ and ‘b’ are given in Fig. 7. The results show that grounding the sheaths on the source side leads to a resonance in voltage magnitude at approximately 20 kHz (Fig. 7). This is due to the cable length of 2 km which behaves as a quarter-wave line at the resonance frequency. The propagation speed of the waveform is calculated using (12):

$$v = \lambda f = 4 l_{cable} f = 1.6 \times 10^8 \text{ m/s} \approx 0.53 c \quad (22)$$

where l_{cable} is the cable’s length and c is the speed of light in vacuum (3×10^8 m/s). The calculated value is in agreement with the literature [2].

When grounding the sheaths on the opposite side of the source only, the resonance effect disappears (Fig. 8). This configuration excites the sheath modes of the underground link which have a different propagation speed that can explain the absence of the resonance.

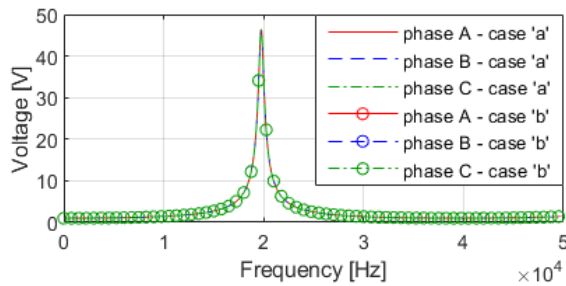


Fig. 7. Frequency response of the no-load 2 km cable with shields grounded on both sides and on the source side (case ‘a’ and ‘b’).

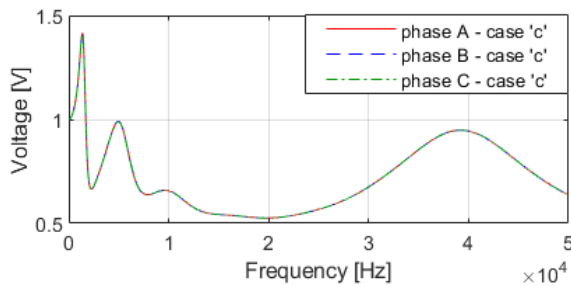


Fig. 8. Frequency response of the no-load 2 km cable with shields grounded on the opposite side of the source (case ‘c’).

B. Investigation of the ‘GIS-transformer-distribution network’ input impedance

The underground cable is connected to the GIS that feeds the power transformer. In order to check the conditions for a quarter-wave resonance in the studied case (Fig. 3), the input impedance of the system connected to the cable is investigated. A frequency scan is performed and the results are given in Fig. 9. At 20 kHz, the input impedance is 3.4 kΩ. When connecting a load of 3.4 kΩ to the cable with sheaths grounded at both ends, the frequency analysis leads to a resonance as can be seen in Fig. 10. Therefore, the system

connected to the underground cable behaves as an open-circuit (high impedance) at 20 kHz that meets the requirements for a quarter-wave resonance as stated in section II.

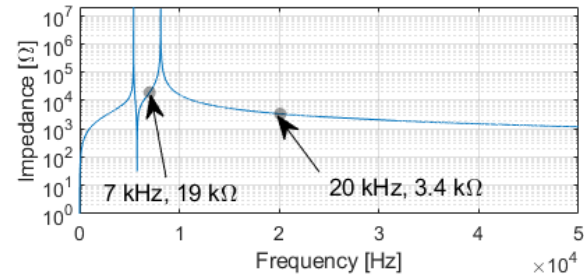


Fig. 9. Input impedance of ‘GIS-transformer-distribution network’ system

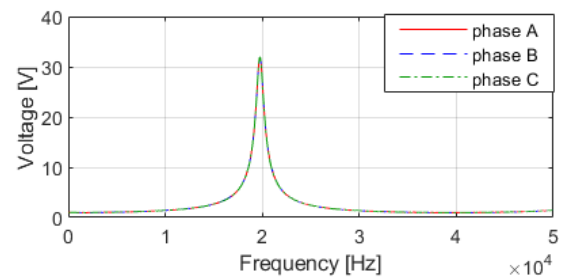


Fig. 10. Frequency response of the 2 km cable with sheaths grounded on both sides and a load of 3.4 kΩ

C. ‘GIS-transformer-distribution network’ frequency analysis

In this paragraph, the system connected to the cable and formed by the GIS, the power transformer and the electric network distribution is analyzed in order to reveal any other resonant frequency that may lead to overvoltages. Hence, a frequency scan is performed by connecting a sinusoidal voltage source with an amplitude of 1 V to the input of the GIS. The phase to ground voltage amplitude at the output of the transformer when supplying phase A is given in Fig. 11. It reflects the transformer gain defined as the ratio of the output to the input voltage (given that the input is 1 V). A resonance appears around 20 kHz and another voltage resonance is detected at 7 kHz. At this frequency, the input impedance is very high and equal to 19 kΩ (Fig. 9). Similar results are obtained with excitation on phase B and C. This may lead to a quarter-wave resonance with a cable of a specific length as will be shown in the next paragraph.

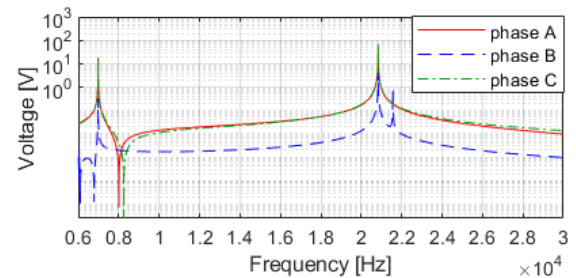


Fig. 11. Frequency response of the ‘GIS-transformer-distribution network’ system with excitation on phase A – Transformer gain ratio

D. Global system overvoltage resonance

At first, the global system described in section III with a 2 km underground cable is studied. Following the lightning

strike, a surge arrester fault is simulated on the one that has the maximum peak voltage. The surge arrester connected to phase A has the maximum voltage of 534.8 kV at 55.1 μ s. It is short-circuited at this instant. The phase to ground voltage observed at the secondary winding of the power transformer is shown in Fig. 12. As mentioned in the previous paragraph, the conditions of a quarter-wave resonance are met. This leads to an overvoltage of 157 kV. This value is higher than the secondary winding lightning withstand voltage (75 kV) even though for the primary winding the overvoltage is below its withstand limit of 900 kV (Fig. 13). The lightning withstand voltage should be seen as an order of magnitude and not as a strict comparison limit due to the difference between the waveform of the lightning test and the simulated overvoltage. In this configuration, EMTP-like simulations showed that adding a surge arrester directly on the HV side of the transformer does not prevent the resonance. The transmitted overvoltage remains very high with a maximum value of 110 kV phase to ground.

In a second step, the cable length is modified to meet the quarter-wave length that corresponds to the resonance frequency of 7 kHz observed for the ‘GIS-transformer-network distribution’. Knowing that the propagation speed is 1.6×10^8 m/s (22), the cable length is changed from 2 km to:

$$l_{cable} = v/4f = 1.6 \times 10^8 / (4 \times 7000) = 5714 \text{ m} \quad (23)$$

Using this length for the underground cable, a resonance is obtained (Fig. 14). An overvoltage of 106 kV is observed on phases A and C. Note that the instant of failure of the surge arrester on phase A is modified to 88 μ s to coincide with the voltage peak of the arrester (485 kV) in this configuration.

As mentioned in section II, a quarter-wave ($\lambda/4$) line also resonates for odd multiples of the quarter wavelength. In order to verify the influence of the length of the cable on the transmitted overvoltage, the length of the cable is modified so that it is equal to $3\lambda/4$ or 17.142 km. With this cable length, a resonance is observed as shown in Fig. 15. However, the overvoltage at the output of the transformer is reduced to 34 kV. In fact, the surge arrester voltage peak at the time of failure is 374 kV (at 233.16 μ s). This peak is much lower than the peak obtained with a shorter cable (5.714 km) which was 485 kV and the transmitted overvoltage was of 106 kV.

TABLE III summarizes the results obtained with the different cable lengths. At a certain length, the cable can have a quarter-wave behavior that causes resonance and oscillatory overvoltage which can reach very high values. Furthermore, the surges transmitted during resonance are higher when the cable length is shorter.

TABLE III
SUMMARY OF THE OVERVOLTAGE RESULTS WITH DIFFERENT
CABLE LENGTHS

Resonance frequency [kHz]	Cable length [km]	Surge arrester peak voltage [kV]	Transmitted overvoltage [kV]
20	2 ($\lambda/4$)	534.8	157
7	5.714 ($\lambda/4$)	485	106
7	17.142 ($3\lambda/4$)	374	34

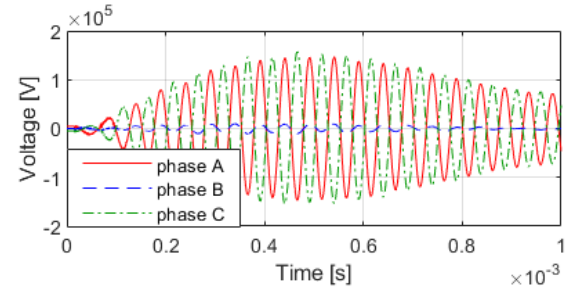


Fig. 12. Phase to ground overvoltage at the secondary winding of the transformer with a 2 km cable

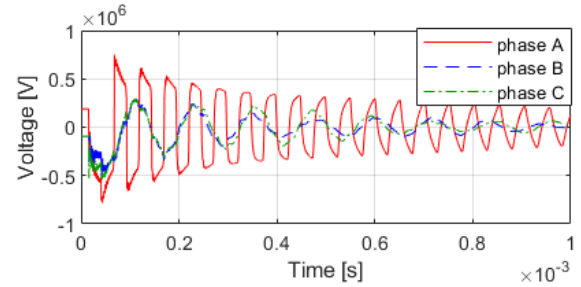


Fig. 13. Phase to ground overvoltage at the primary winding of the transformer with a 2 km cable

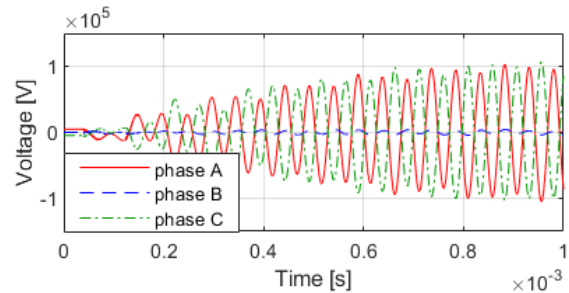


Fig. 14. Phase to ground overvoltage at the secondary winding of the transformer with a 5.714 km cable

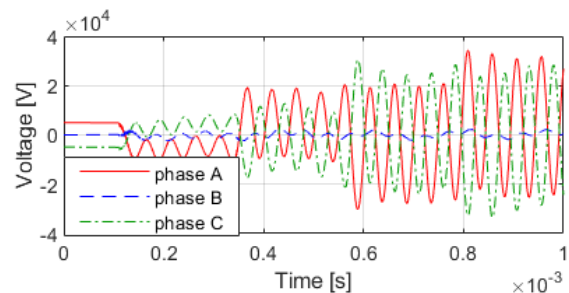


Fig. 15. Phase to ground overvoltage at the secondary winding of the transformer with a 17.142 km cable

E. Effect of the load on the resonance frequency

The studied system may feed variable loads. For example, when supplying a production facility, the load during the day (industrial machines, fans, conveyers, etc...) might be higher than that during the night (minimal load for lighting and emergency systems). Thus, the effect of the load is investigated in this paragraph. A PQ-load (600 kW, 290 kVAR) and a phase to ground capacitance (46 nF) are used to model a medium voltage motor connected to the distribution network fed by the transformer. The presence of

the load changes the frequency response of the GIS-transformer system. Fig. 16 shows the phase to ground voltage at the output of the transformer with the phase A of the GIS excited using a 1 V sinusoidal source. There is no resonance detected in the system. Time domain simulation is performed on the global system using a 2 km underground cable with the load connected. The overvoltage at the transformer secondary winding is very low with a peak of 20 kV. It is significantly lower than the secondary winding lightning withstand voltage (75 kV).

In order to better understand the effect of the load on the maximum overvoltage, other medium voltage PQ-load values are considered. The power factor is fixed to 0.9 and three active power P are simulated: 1 kW, 100 kW and 1000 kW. The results are summarized in TABLE IV. When the load is low, the overvoltage can be very high (115 kV). Even at 100 kW, the overvoltage (60 kV) has the same order of magnitude of the secondary winding lightning withstand voltage (75 kV). When the load is sufficiently high, the overvoltage is very low (15 kV) and the risk of damage due to severe overvoltage is eliminated.

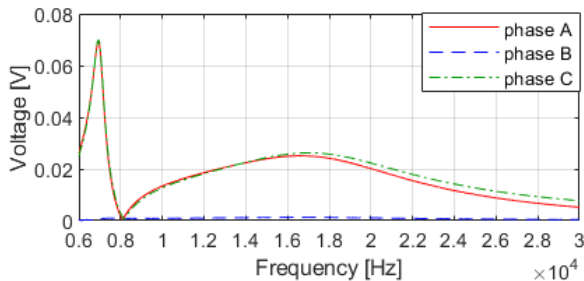


Fig. 16. Frequency response of the ‘GIS-transformer’ system with excitation on phase A – Transformer gain ratio with load

TABLE IV
MAXIMUM OVERVOLTAGE FOR DIFFERENT LOAD VALUES

Active power of the load [kW]	Transmitted overvoltage [kV]
1	115
100	60
600	20
1000	15

V. CONCLUSION

In this paper the overvoltage due to the resonance that appears as a result of the high frequency interaction between a quarter-wave cable and a power transformer is presented and analyzed. The theoretical background about transmission lines and the conditions of a quarter-wavelength resonance are presented. The case of a lightning strike with a surge arrester fault is considered and the high frequency models of the system components are detailed.

The different resonance frequencies of the system are investigated. The results showed that the cable with a certain length can behave as a quarter-wave line at specific frequencies. This phenomenon may lead to high overvoltage at the secondary winding of the power transformer even if at the

primary side they are well below the lightning withstand voltage of the equipment. In this configuration, EMTP-like simulations showed that adding a surge arrester directly on the high voltage side of the transformer does not significantly reduce the transmitted resonance overvoltage.

The connection of the load modifies the frequency response of the GIS-transformer-distribution network system and can eliminate the risk of appearance of these critical overvoltages.

VI. REFERENCES

- [1] B. Filipović-Grčić, B. Franc, I. Uglešić, I. Pavić, S. Keitoue, I. Murat, I. Ivanković, “Monitoring of transient overvoltages on the power transformers and shunt reactors – field experience in the Croatian power transmission system”, *Procedia Engineering* 202, pp.29–42, 2017
- [2] A. Holdyk, B. Gustavsen, “External and Internal Overvoltages in a 100 MVA Transformer during High-Frequency Transients”, *International conference on Power Systems Transients (IPST)*, Cavtat, Croatia, June 2015.
- [3] CIGRE Technical Brochure 577A, “Electrical transient interaction between transformers and the power system – Part 1 – Expertise”, 2014
- [4] J. Snodgrass, L. Xie, « Overvoltage analysis and protection of lightning arresters in distribution systems with distributed generation, *Electrical Power and Energy Systems* 123, 2020
- [5] R. Oliveirs; P. Bokoro; W. Doorsamy, « Investigation of Very Fast-Front Transient Overvoltages for Selection and Placement of Surge Arresters”, 2018 *Power Systems Computation Conference (PSCC)*, Dublin, Ireland, 2018
- [6] CIGRE Technical Brochure 577B, “electrical transient interaction between transformers and the power system – Part 2: Case studies, 2014
- [7] X. Zhao, J. Li, L. Pu, Z. Ju, S. Ren, W. Duan, H. Sun, M. Fan, X. Chen, J. Deng, “Transient Overvoltage in 10kV Hybrid OHL-Cable System during Energization”, 2018 *IEEE International Conference on High Voltage Engineering and Application (ICHVE)*, Athens, Greece, 2018.
- [8] J.A. Santiago, M.C. Tavares, « Electromagnetic Transient Study of a Transmission Line Tuned for Half Wavelength”, *International conference on Power Systems Transients (IPST)*, Cavtat, Croatia, June 2015.
- [9] F. Proença, R. Pereira, E. Costa; L.H. Liboni, "Overvoltage Suppression in Half-Wavelength Transmission Systems using Line Surge Arresters », 2019 *International Symposium on Lightning Protection (XV SIPDA)*, São Paulo, Brazil, 2019
- [10] B. Gustavsen, “Study of Transformer Resonant Overvoltages Caused by Cable-Transformer High-Frequency Interaction”, *IEEE Transactions on Power Delivery*, Vol. 25, No. 2, April 2010
- [11] IEC 60071-1, “Insulation co-ordination: Definitions, principles and rules”, 2019
- [12] K. Zhang, D. Li, “Transmission-Line Theory and Network Theory for Electromagnetic Waves. In: *Electromagnetic Theory for Microwaves and Optoelectronics.*” Springer, Berlin, Heidelberg, 2008, pp.117-178.
- [13] EMTP, <https://www.emtp-software.com/>
- [14] IEC 60071-4, “Insulation co-ordination: Computational guide to insulation co-ordination and modelling of electrical networks”, 2014
- [15] F. Heidler, Z. Flisowski, W. Zischank, Ch. Bouqueneau, C. Mazzetti, «Parameters of lightning current given in IEC 62305 – background, experience and outlook», 29th *International Conference on Lightning Protection*, Uppsala, Sweden, June 2008.
- [16] IEC 62305-1, “Protection against lightning: General principles”, 2010.
- [17] H. W. Dommel, “Digital computer solution of Electromagnetic Transients in single and multiphase networks”, *IEEE Transactions*, Vol. PAS-88, pages 388-399, April 1969
- [18] J. Marti: “Accurate Modeling of Frequency Dependent Transmission Lines in Electromagnetic Transient Simulations”, *IEEE Trans. On Power Apparatus and Systems*, vol. PAS-101, pp. 147-157, 1982.
- [19] L. Marti: “Simulation of transients in underground cables with frequency-dependent modal transformation matrices”. *IEEE Trans. in Power Delivery*, Vol. 3, Issue: 3, July 1988, pp. 1099 -1110.
- [20] G. R. Slemon, “Equivalent circuits for transformers and machines including non-linear effects,” *Proc. Inst. Elect. Eng.*, vol. 100, pt. IV, pp. 129-143, 1953.
- [21] B. Jurisic, I. Uglešic, A. Xémard, F. Paladian, “Difficulties in high frequency transformer modeling”, *Electric Power Systems Research*, Vol. 138, September 2016, pp. 25-32.